Per. Mineral. (2001), *70*, 3, 377-386 http://go.to/permin

PERIODICO di MINERALOGIA
established in 1930

An International Journal of
MINERALOGY, CRYSTALLOGRAPHY, GEOCHEMISTRY, ORE DEPOSITS, PETROLOGY, VOLCANOLOGY
and applied topics on *Environment, Archaeometry* and *Cultural Heritage*

Kelyphitic breakdown of garnets from pyroxenite xenoliths, south-eastern Sicily, Italy.

GIOVANNA SAPIENZA[1], VITTORIO SCRIBANO[1]* and SONIA CALVARI[2]

[1] Dipartimento di Scienze Geologiche dell'Università, Corso Italia 55, I-95129 Catania, Italy
[2] Istituto Nazionale di Geofisica e Vulcanologia, Piazza Roma 2, I-95124 Catania, Italy

Submitted, May 2001 - Accepted, September 2001

ABSTRACT. — Upper-mantle garnet-pyroxenite xenoliths rarely occur in Miocene basaltic diatremes from the Hyblean Plateau, SE Sicily (Italy). Three representative samples from Valle Guffari tuff-breccia deposits are examined here. A subsolidus origin for garnet may be invoked for two of these samples (one spinel-garnet websterite, UL-c17; one garnet-spinel-orthopyroxene clinopyroxenite, UL-d47). In the third sample (a garnet clinopyroxenite, UL-d21), which has mineral compositions similar to those of sample UL-d47, garnet is a cumulus product.

Garnet appears partially replaced by an optically unresolvable mineral intergrowth (kelyphite) which, under SEM (EDS), turns out to be composed of Ca-poor pyroxene, spinel and Ca-plagioclase. Kelyphite bulk compositions, obtained by automatic raster analyses, closely match their relative garnet mineral chemistry. This fact and mass balance calculations suggest a near-isochemical garnet breakdown process, primarily controlled by an increase in temperature and decompression, as a consequence of xenolith entrainment into the host magma and ascent to the surface, although a catalysing effect by fluids was very probable at any stage of the process.

RIASSUNTO. — Fra gli xenoliti mantellici dei diatremi basaltici di età Miocenica degli Iblei (Sicilia), sono stati segnalati diversi tipi di pirosseniti a granato; questo è parzialmente, talora totalmente, sostituito da kelifite torbida fino ad opaca, otticamente irrisolvibile. È stata condotta un'indagine al SEM su questi prodotti di trasformazione, tesa a chiarire alcuni aspetti delle ultime fasi della storia sub-solidus di tali rocce.

Sono stati selezionati tre campioni rappresentativi: una websterite a spinello e granato (UL-c17), una clinopirossenite a granato con poco spinello e raro ortopirosseno (UL-d47) e una clinopirossenite a granato (UL-d21). A dispetto della originaria accezione del termine «kelifite» (reazione coronitica), nei campioni studiati non si hanno zonature concentriche della stessa. Essa aggredisce il minerale con andamento cellulare: da micro-fratture, che suddividono il cristallo in poliedri irregolari, si propaga verso il centro dei poliedri.

Nonostante le sensibili differenze petrografiche fra i campioni, in tutti coesistono zone kelifitiche a diversa tessitura e simile composizione mineralogica (pirosseni poveri in calcio, spinelli, Ca-plagioclasi). Le differenze tessiturali riguardano principalmente la grana, l'allungamento e la disposizione spaziale dei minerali della kelifite: è stata distinta una kelifite (K1) con disposizione a covone di gruppi di minerali fibrosi (1-5 μm × 10-25 μm); irregolarmente disperse in questa, si trovano sacche kelifitiche (K2) ove i minerali, marcatamente inequigranulari (5-45 μm) non sono generalmente allungati.

La composizione chimica *in toto* della kelifite fine

* Corresponding author, E-mail: scribano@unict.it

ottenuta in automatico (raster) su aree di 75 μm^2 mima quella del granato originario. Anche calcoli di bilanci di massa concorrono ad indicare che nel nostro caso la trasformazione kelifitica è tendenzialmente isochimica. Questo breakdown è dovuto ed aumento di temperatura e decompressione in seguito alla risalita del magma ospite e all'intrappolamento dello xenolite, ma non si può escludere l'azione catalizzatrice di fasi fluide ad ogni stadio del processo.

KEY WORDS: *Sicily, xenoliths, pyroxenite, garnet, kelyphite.*

INTRODUCTION

Some basanitic breccia pipes from the Hyblean Plateau (SE Sicily, Italy) bear a number of deep-seated xenoliths representing various lithologies of the lithospheric column (Punturo *et al.*, 2000, and references therein). The mantle xenoliths consist of spinel-facies peridotite and several types of pyroxenite. These sometimes contain variable quantities of garnet, which is either partially or totally replaced by an optically unresolvable «kelyphite» (this term is here used in a non-genetic sense). A SEM study on kelyphite mineral compositions and texture will provide further information on the last stage of the subsolidus history of these garnet-bearing pyroxenite xenoliths. Three representative garnet-bearing pyroxenites from Valle Guffari (fig. 1) are examined here.

ESSENTIAL PETROGRAPHIC AND GEOCHEMICAL FEATURES OF GARNET-BEARING PYROXENITE XENOLITHS

The petrographical characteristics of the examined samples are listed in Table 1. In detail, sample UL-c17 consists of a spinel-garnet websterite exhibiting xenomorphic granular texture due to coarse (4-5 mm) equant clinopyroxene grains, abundant inequigranular greyish-green spinel, subordinate Ca-poor pyroxene, and a little coronitic garnet. It occurs between spinel and coexisting pyroxenes. Clinopyroxene shows notable exsolution lamellae of Ca-poor pyroxene. The mineral chemistry of the consituent minerals of sample Ul-c17 is reported in Table 2.

Sample UL-d47 is a garnet-spinel-

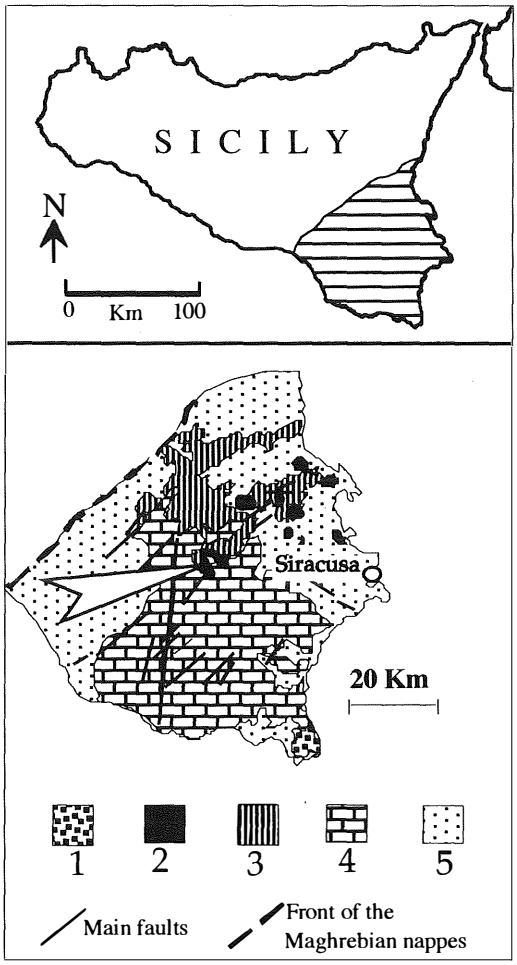

Fig. 1 – Geological sketch map of Hyblean region and location of Valle Guffari (arrow), where examined garnet-bearing xenoliths were found. 1: Upper Cretaceous lava flows and dikes (alkaline basalt). 2: Upper Miocene tuff-breccia deposits and subordinate lava flows (alkaline basalt, nephelinite). 3: Plio-Pleistocene lava flows (tholeiite and alkaline basalt, basanite, nephelinite, hawaiite). 4: Mesozoic-Cenozoic deep-water carbonates. 5: Neogene-Quaternary open shelf clastics.

TABLE 1

Petrographic characteristics of examined garnet-bearing pyroxenite xenoliths.

Sample	**Lithotype**	**Colour**	**Texture and constituent minerals**	**Xenolith shape, size, weight**
UL-c17	Spinel-garnet websterite	Greenish grey	Xenomorphic granular. Coarse (5mm) equant Al-diopsidic *cpx*, *opx*, Al-spinel, scarce reaction garnet.	Rounded 8 cm ca. 840 gr
UL-d47	Garnet-spinel-orthopyroxene clinopyroxenite	Dark grey	Adcumulitic with neoblastic zones. Subhedral megacrystic (> 2 cm) Al-*cpx*, anhedral garnet (35 vol%), Al-spinel, magnetite, subordinate Ca-poor pyroxene.	Ovoid 12×8 cm ca 1220 gr.
UL-d21	Garnet clinopyroxenite	Dark grey	Cumulitic. Megacrystic (> 2 cm) Al-*cpx*, subordinate coarse (5 mm) cumulus garnet.	Irregular with rounded edges $8 \times 6 \times 3$ cm ca. 550 gr.

orthopyroxene clinopyroxenite with elongated, very coarse (2-10 cm long), subhedral clinopyroxene crystals enclosing rare, etherogranular spinel grains. Scarce orthopyroxene occurs between the larger calcic pyroxene crystals. The clinopyroxene grains appear to be irregularly interlocked with anhedral garnet. The garnet encloses a number of rounded, clinopyroxene micro-grains exhibiting incoherent extinction and the same chemical composition as the coexisting clinopyroxene oikocrysts. Rare, rounded, opaque Al-spinel relics are also enclosed in the garnet. The chemistry of these minerals is reported in Table 2.

Spinel is missing in the garnet-clinopyroxenite xenolith UL-d21, which has cumulate texture with rare, euhedral garnet grains and subhedral clinopyroxene oikocrysts. The mineral chemistry of both garnet and pyroxene is very similar to corresponding phases from sample UL-d47, except for CaO and FeO (Table 2). In addition, pyroxene oikocrysts from UL-d21 have irregular composizional zoning (e.g., CaO varies from 14.5 to 16.5 wt%; TiO_2 from 1.1 to 1.5 wt%: cf. Table 2). Post-entrainment modifications, as well as partially melted glassy patches, spongy zones in the Ca-pyroxene, and decompression micro-cracks in garnet, are ubiquitous in these xenoliths, especially in sample UL-d21.

Major element and REE whole-rock distributions in the samples are listed in Table 3. It is worth noting that samples UL-d47 and UL-d21, although having very similar mineral chemistry, show different whole-rock compositions, due to diverse modal distribution of spinel and/or garnet.

TABLE 2

Representative mineral chemistry of examined samples. Cpx-1 and Cpx-2 represent compositional variations in UL-d21 clinopyroxene. Symbols of minerals after Kretz (1983).

	UL-c17 Cpx	UL-c17 Opx	Ulc-17 Spl	UL-c17 Grt
wt%				
SiO_2	51.27	54.15	0.00	40.36
Al_2O_3	4.80	3.31	60.01	22.62
TiO_2	0.80	0.07	0.21	0.11
FeO(*tot*)	5.27	13.09	21.88	16.16
MnO	0.07	0.18	0.10	0.46
MgO	14.73	29.37	16.52	14.12
CaO	23.18	0.53	0.00	6.75
Na_2O	0.61	0.02	0.00	0.03
Total	100.72	100.74	98.73	100.61
	UL-d47 Cpx	UL-d47 Opx	UL-d47 Spl	UL-d47 Grt
wt%				
SiO_2	48.48	51.23	0.09	40.89
Al_2O_3	9.52	6.89	59.78	22.71
TiO_2	1.59	0.54	0.56	0.56
FeO(*tot*)	7.81	12.53	20.35	13.17
MnO	0.08	0.19	0.11	0.28
MgO	13.54	27.20	18.02	16.92
CaO	17.81	1.35	0.00	5.57
Na_2O	1.41	0.18	0.00	0.00
Total	100.36	100.12	99.02	100.09
	UL-d21 Cpx-1	UL-d21 Cpx-2	UL-d21 Cpx-3	UL-d21 Grt
wt%				
SiO_2	48.8	48.15	48.79	39.91
Al_2O_3	9.78	9.81	7.23	21.68
TiO_2	1.13	1.49	1.56	0.81
FeO(*tot*)	9.99	8.77	8.03	15.23
MnO	0.00	0.23	0.00	0.34
MgO	13.60	13.50	15.10	15.20
CaO	14.77	16.54	19.32	5.47
Na_2O	1.59	1.38	0.50	0.00
Total	99.66	99.87	100.03	98.64

TABLE 3

Whole-rock chemistry (major elements and REE) of garnet-bearing pyroxenite xenoliths. mg=MgO/(MgO+FeO_{tot}) mol%. Analytical data after Punturo and Scribano (1997) for sample UL-c17 and Sapienza and Scribano (2000) for samples UL-d47 and UL-d21.*

	UL-d47	UL-d21	UL-c17
wt%			
SiO_2	43.91	48.05	44.18
Al_2O_3	14.57	8.42	11.17
TiO_2	1.22	0.85	1.5
FeO(*tot*)	9.38	9.88	7.51
MnO	0.17	0.17	0.11
MgO	14.17	15.7	14.41
CaO	12.34	13.69	15.93
Na_2O	1.14	1.06	0.76
K_2O	0.13	0	0.09
P_2O_5	0.18	0.04	0.11
CO_2	0.13	0.08	0.11
H_2O	1.87	0.87	2.97
Total	99.38	98.91	99.22
mg*	0.60	0.61	0.66
ppm			
La	4.4	0.8	7.8
Ce	10.8	3.1	18.0
Pr	1.6	0.6	n.d.
Nd	8.2	3.9	12.0
Sm	2.6	1.8	3.3
Eu	1.1	0.6	1.3
Gd	3.3	2.5	nd
Tb	0.6	0.4	0.6
Dy	4.8	2.5	nd
Ho	1.1	0.5	nd
Er	3.0	1.2	nd
Tm	0.5	0.2	nd
Yb	3.7	1.0	1.2
Lu	0.6	0.2	0.2
Sm*/Yb*	0.7	1.9	2.9

Sample UL-c17 has a relatively high Sm_n/Yb_n ratio (= 2.9; Table 3, fig. 2), which may be ascribed to cryptic metasomatism (Sapienza and Scribano, 2000). Instead, sample UL-d47 displays evident HREE fractionation (Sm_n/Yb_n = 0.7; Table 3, fig. 2), probably due to the relatively high modal proportion of garnet (35 vol%). Lastly, the upward-convex

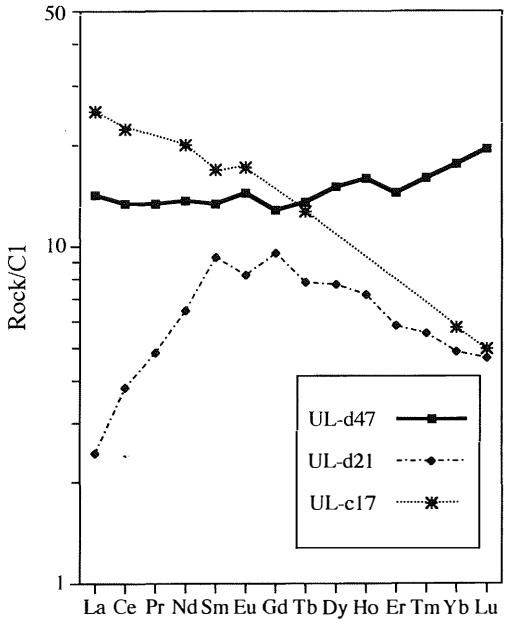

Fig. 2 – C1-normalized REE patterns for garnet-bearing pyroxenite xenoliths. Normalizing values after Boynton (1984).

REE pattern of sample UL-d21 (fig. 2) suggests a cumulus origin, on the basis of its texture (Table 1).

TEXTURE AND MINERAL CHEMISTRY OF KELYPHITE

Kelyphite texture

Kelyphite replacing garnet appears as an optically unresolvable, brownish, birefringent mat with indistinct interference colours. The radial-type extinction suggests the fibrous nature of its constituent minerals. In addition, the extinction patterns indicate that relatively large areas of kelyphite consist of a number of closely juxtaposed, differently oriented domains with gently curved boundaries. They represent micro-cracks of the original garnet grains (fig. 3). Hence, kelyphitization proceeds along main cracks, groups of kelyphite fibrous minerals being coaxially arranged normally to the crack walls. This type of turbid, brownish, kelyphite hosts variable quantities of irregular, opaque patches.

Back-scattered electron images by SEM distinguish two coexisting kelyphite textures, the first (K1) consisting of an extremely fine intergrowth of irregular rods (1-5 μm wide, 10-25 μm long) of Ca-poor pyroxene, spinel and Ca-plagioclase (fig. 4a,b). SEM observations also confirm that the optically perceivable kelyphite domains consist of clusters of low-angle convergent elongated crystals (fig. 4c).

The second kelyphite texture (K2) consists of striking inequigranular (5-45 μm) intergrowths of platey crystals of Ca-poor pyroxene, oxides (Al-spinel and Ti-magnetite) and Ca-plagioclase. More precisely, the oxides, significantly finer than the coexisting silicates, in most cases appear enclosed in the pyroxene (fig. 5a,b). The transition between K1 and K2 is very irregular and the two kelyphite types often appear slightly interfingered (fig. 5b). The volume proportions between the two types vary greatly on the thin-section scale.

The sub-kelyphite surfaces on garnets from

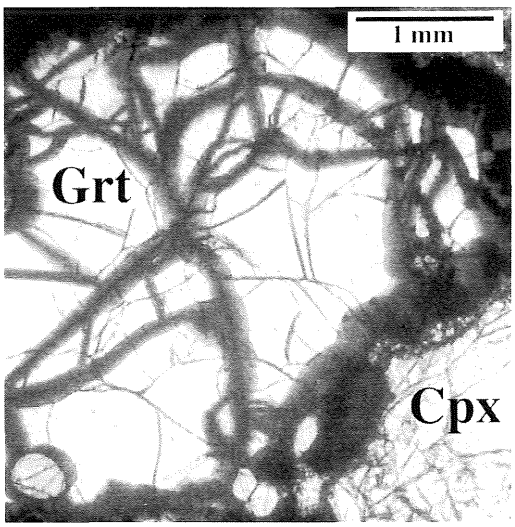

Fig. 3 – Microphotograph (plane pol. light) of one partially kelyphitized garnet grain from UL-d47 pyroxenite xenolith. Kelyphite (very dark in photo) emphasizes irregular cracks in garnet.

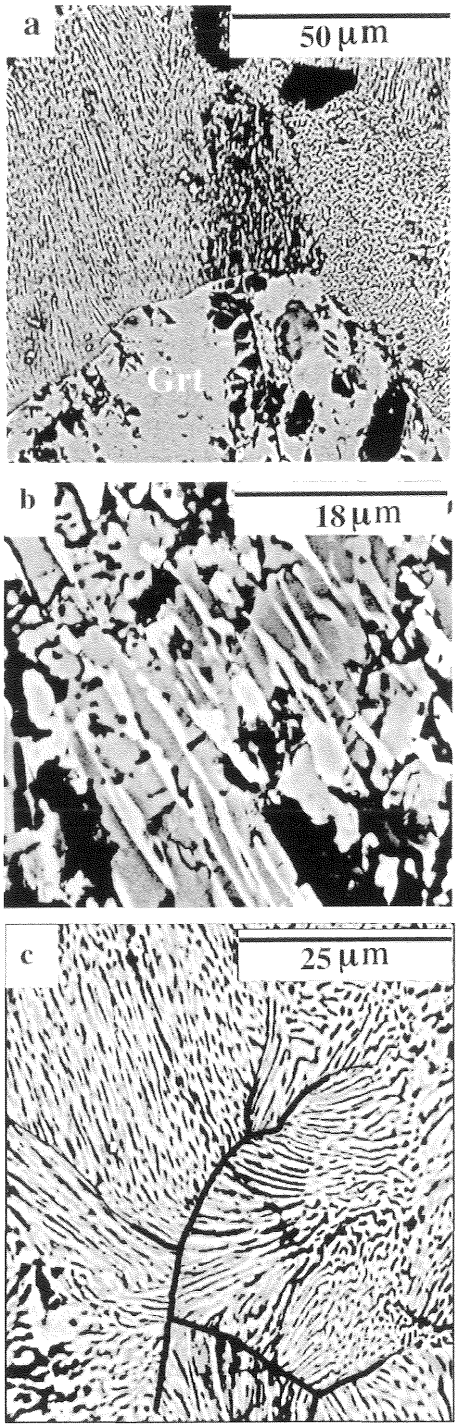

all three samples show a number of evenly distributed 1-5-μm pits, irregular elongated shape, and generally curvilinear edges.

Kelyphite mineral chemistry

Minerals from K1 kelyphites expose surfaces no larger than the beam area in most cases. However, the close intergrowth of such fine crystals does not allow reliable estimates of their relative volume proportions, although automatic raster analyses on 75-μm^2 areas of K1 kelyphite closely match the chemical compositions of the relative original garnets.

Instead, the relatively coarser K2 kelyphite minerals permit systematic spot analyses and rough estimates of their relative volume percentages: Ca-poor pyroxenes are the dominant phase in all samples, oxides being subordinate to coexisting silicates (e.g., fig. 5).

Although the constituent minerals of kelyphite exhibit significant, irregular compositional zoning, our data set does allow us to estimate a probable weighted average composition (on the basis of a minimum of 15 quality analyses) for each mineral phase reported in Table 4.

DISCUSSION

Partial kelyphite replacement of Mg-rich garnets from worldwide mantle rocks is ubiquitous. Many authors use the term to indicate corona reactions surrounding garnet, according to the original meaning of the Greek word *kelyphos* (rind, shell; e.g., Garvie and

Fig. 4 – SEM images of fibrous kelyphite type (K1) in studied samples. *a*) Bottom half of figure: part of garnet relict with pitted sub-kelyphite surface. Right: coaxially arranged K1 minerals are cut perpendicularly to elongation axes (sample UL-d47); *b*) Magnification of K1 kelyphitic intergrowth in sample UL-d47: Ca-plagioclase (dark-grey), Ca-poor pyroxene (medium-grey), Al-spinel and magnetite (whitish); *c*) Low-angle convergence of groups of elongated K1 minerals, pattern being controlled by irregular micro-cracks (inked in photo) of original garnet (sample UL-c17).

TABLE 4

Kelyphite mineral chemistry. Variation intervals and weighted averages (calculated on basis of minimum 15 analyses) are reported for each mineral phase. Equipment: Cambridge SEM fitted with EDS probe (operative conditions: 1.5 KV, current beam 20 nA, live time 100s, ZAF corrections) at Istituto Nazionale di Geofisica e Vulcanologia, Catania.

KELYPHITE OXIDES

	UL-c17		UL-d47		UL-d21	
	Variation	Average	Variation	Average	Variation	Average
wt%						
SiO_2	0.00 – 0.31	0.08	0.00 – 0.50	0.00	0.00 – 0.61	0.31
Al_2O_3	0.76 – 63.41	46.40	5.83 – 62.69	47.16	9.77 – 62.88	45.93
TiO_2	0.00 – 52.83	5.96	0.00 – 24.52	5.62	0.00 – 18.90	6.51
FeO(*tot*)	18.19 – 64.76	34.21	22.42 – 64.31	34.77	20.09 – 63.24	33.92
MnO	0.22 – 0.59	0.2	0.00 – 0.67	0.33	0.00 – 0.58	0.31
MgO	5.29 – 17.46	13.15	5.27 – 14.95	12.12	5.17 – 16.33	13.02
Total		100.00		100.00		100.00
mg*	0.16 – 0.60	0.40	0.19 – 0.54	0.38	0.17 – 0.63	0.40

KELYPHITE PYROXENES

	UL-c17		UL-d47		UL-d21	
	Variation	Average	Variation	Average	Variation	Average
wt%						
SiO_2	48.89 – 54.64	52.40	46.52 – 50.92	47.68	46.47 – 49.94	47.50
Al_2O_3	12.43 – 2.90	4.26	7.98 – 13.53	12.41	8.50 – 14.31	11.40
TiO_2	0.00 – 1.71	0.96	0.26 – 0.56	0.31	0.25 – 0.50	0.41
FeO(*tot*)	11.77 – 15.12	13.62	13.64 – 16.96	14.35	15.28 – 17.08	16.30
MnO	0.00 – 0.63	0.29	0.00 – 0.47	0.38	0.00 – 0.65	0.50
MgO	22.70 – 29.96	27.12	22.51 – 25.92	22.73	21.82 – 22.73	22.20
CaO	0.41 – 2.26	1.35	1.23 – 2.77	2.14	1.33 – 2.05	1.69
Total		100.00		100.00		100.00
mg*	0.73 – 0.81	0.78	0.71 - 0.77	0.74	0.70 – 0.71	0.71

KELYPHITE FELDSPARS

	UL-c17		UL-d47		UL-d21	
	Variation	Average	Variation	Average	Variation	Average
wt%						
SiO_2	45.87 – 47.10	45.21	46.27 – 48.39	47.72	44.52 – 45.60	45.07
Al_2O_3	33.30 – 35.59	34.56	31.50 – 33.22	32.66	33.87 – 34.23	33.92
FeO(*tot*)	0.00 – 1.25	0.84	0.91 – 1.21	1.06	1.33 – 1.53	1.70
MgO	0.00 – 0.00	0.00	0.00 – 0.25	0.12	0.22 – 0.37	0.30
CaO	17.93 – 19.77	18.70	15.49 – 17.22	16.35	18.43 – 18.84	18.64
Na_2O	0.00 – 1.30	0.69	1.38 – 2.43	1.90	0.26 – 0.47	0.37
K_2O	0.00 – 0.00	0.00	0.11 – 0.27	0.19	0.00 – 0.00	0.00
Total		100.00		100.00		100.00
An (mol%)	88 – 100	93	74 – 86	82	93 – 97	96

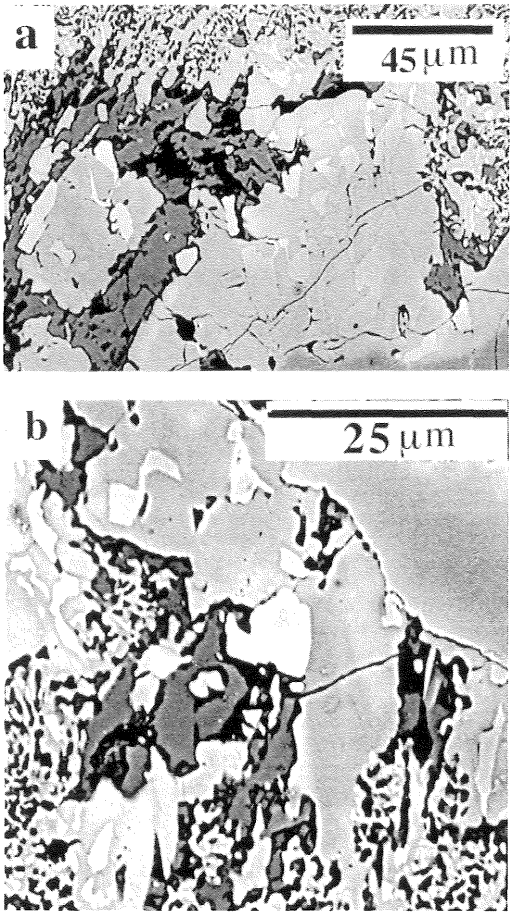

Fig. 5 – SEM images of platey textured kelyphite (K2) in samples UL-c17 (a) and UL-d21 (b). Irregular transition to K1 is also shown. Ca-plagioclase (dark-grey), Ca-poor pyroxene (medium-grey), Al-spinel and magnetite (whitish).

Robinson, 1984, Obata, 1994), although «kelyphite» is also used to indicate extremely fine symplectite intergrowths caused by isochemical garnet breakdown (e.g., Harley *et al.*, 1990)

In our kelyphite samples, there is no evidence of chemical or textural concentric zoning. Moreover, the lack of significant ion exchanges between adjacent mineral phases is proven by the congruity of SEM raster analyses on fine kelyphite areas (K1) from all samples and the relative garnet compositions. In addition, mass balance calculations based on averaged mineral chemistry data on K2 mineral phases (Table 4) support this consideration in two cases (UL-d47, UL-d21: 1 garnet $\rightarrow$ 0.15 *ox* + 0.6 *px* + 0.25 *pl*). Conversely, the garnet breakdown reaction may be not strictly isochemical in sample UL-c17, since TiO_2 and Na_2O are missing in the original garnet but are present in the calculated one. Also, CaO is 5.35 wt% in the original garnet but 6.96 wt% in the calculated one.

Optical observations in our samples indicate that garnet kelyphitization proceeds along irregular, anastomosing cracks (fig. 3), which depend on the lack of structural anisotropy in garnet and may be enhanced by decompression, probably during xenolith ascent to the surface. The inward, cellular progress of kelyphite transformation observed here may depend on the temperature gradient: some experimental data show that ultramafic xenoliths up to 10 cm in diameter are heated to the temperature of the host magma within three hours of entrainment (Selverstone, 1982).

Garvie and Robinson (1984) invoke the effect of a temperature gradient and thus of a different ion diffusion rate, to explain grain-size differences in kelyphite constituent minerals. This interpretation may also fit the mineral-size difference observed by us in K1 and K2 kelyphite textural types. Nevertheless, in our case, there is no evidence of a regular concentric distribution of «coarse» and «fine» kelyphites as described by the above-mentioned authors. This textural difference may be favoured by gases from decrepitated fluid inclusions in garnets: such local enrichment in volatiles (CO_2?) may inhibit further nucleation, enhance the ion diffusion rate and thus favour the growth of previously formed kelyphite minerals. In addition, some of the already described pits on sub-kelyphite garnet surfaces may represent dissected fluid inclusions, although Garvie and Robinson (1984) consider similar pits as roots of kelyphite elongated pyroxene crystallites. However, the major role of fluids in the formation of kelyphite appears unlikely, since

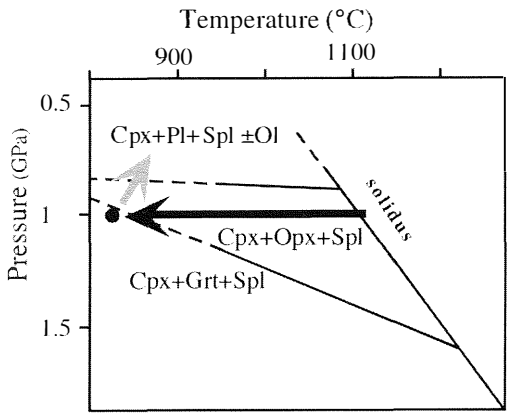

Fig. 6 – Probable isobaric cooling path (long arrow) for sample UL-c17 and possible post-entrainment, kelyphite-forming trend (short arrow). Sample plotting (circle) after P-T estimates (for full explanation, see text). Subsolidus phase relationships for garnet websterite R394 (Australia) from Irving (1974).

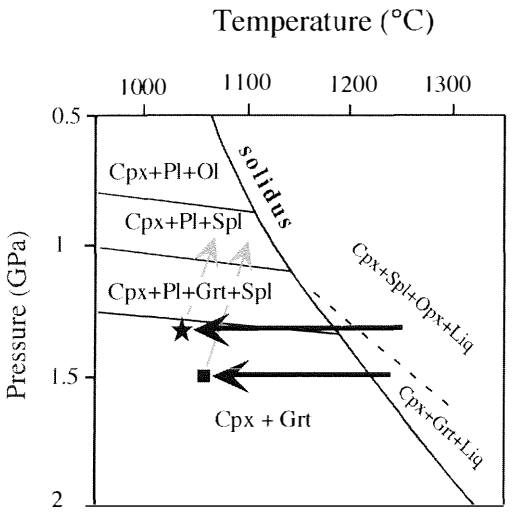

Fig. 7 – Suitable isobaric cooling paths (heavy arrows) for samples UL-d47 and UL-d21 and relative post-entrainment, kelyphite-forming trends (light arrows). Sample plotting (UL-d47, star; UL-d21, square) according to P-T estimates (for full explanation, see text). Subsolidus phase relationships for garnet clinopyroxenite R392 (Australia) from Irving (1974).

hydrated phases were not found in the samples.

In any case, the formation of kelyphite is related to changing thermo-baric conditions in garnet-bearing rocks. Atzori *et al.* (1999) suggest that sample UL-c17 (spinel-garnet-websterite) represents the complete subsolidus equilibration and annealing of an hypothetical igneous protolith (probably a bi-mineral cumulate of Al-rich, subcalcic clinopyroxene and subordinate Al-spinel), due to isobaric (P=1 Gpa ca.) adaptation to the conductive geotherm. The garnet-forming reaction records the last equilibration temperature (T=740°C) prior to xenolith entrainment into the host magma. In addition, the mineral chemistry of sample UL-d47 suggests an equilibration pressure of 1.32 Gpa and temperature of 1040°C (Atzori *et al.*, 1999). On the basis of UL-d21 averaged clinopyroxene and garnet compositions, we estimate T=1060°C using the garnet-clinopyroxene Fe-Mg geothermometer (Krogh, 1988) and P=1.5 Gpa following Nimis and Ulmer (1998).

These equilibration *loci* were compared with subsolidus phase relationships experimentally determined by Irving (1974) for spinel-garnet websterite xenolith R394 and garnet pyroxenite R392 from Delegate Pipe (SE Australia). The first shows close petrographic and mineralogical similarities to sample UL-c17 and the second to samples UL-d47 and UL-d21, except for differing Mg/Fe ratios and other minor geochemical differences. Therefore, information on the crystallisation histories of our rocks on the basis of Irving's data must be assumed as qualitative only.

Fig. 6 shows a probable garnet-forming isobaric cooling path for UL-c17 (heavy arrow) and a possible post-entrainment P-T path (light arrow), compared with the subsolidus phase relationships experimentally determined by Irving (1974) for spinel-garnet websterite xenolith R394. Hence, fig. 7 displays cooling paths (heavy arrows) for UL-d47 (star) and UL-d21 (square), followed by possible post-entrainment decompression and heating trends (light arrows), compared with experimental data on garnet pyroxenite R392.

CONCLUDING REMARKS

The kelyphite replacement of garnet from three studied pyroxenite xenoliths represents an isochemical breakdown due to an increase in temperature and pressure release, both before and after xenolith entrainment into the host magma. The catalysing effect caused by fluids at any stage of the process is also very probable. In addition, the abrupt loss of thermal energy caused by rapid expansion of volatiles during diatreme eruption halts any breakdown reactions in high-pressure minerals. This fact also accounts for the survival of garnet relics, which would have been more extensively resorbed in the case of normal lava flow emplacement.

ACKNOWLEDGMENTS

Constructive criticism by Prof. F. Innocenti is gratefully acknowledged. Financial support was provided by the Università di Catania (Ricerche di Ateneo 2000-2001).

REFERENCES

ATZORI P., MAZZOLENI P., PUNTURO R. and SCRIBANO V. (1999) — *Garnet-spinel-pyroxenite xenoliths from Hyblean Plateau (South-eastern Sicily, Italy)*. Mineral. Petrol., **66**, 215-226.

BOYNTON W.V. (1984) — *Geochemistry of the rare earth elements: meteorite studies*. In: «*Rare earth elements geochemistry*» Henderson P. (Ed.), Elsevier, 63-114.

GARVIE O.G. and ROBINSON D.N. (1984) — *The formation of kelyphite and associated sub-kelyphitic and sculptured surfaces on pyrope from kimberlite*. In: «Kimberlites I: kimberlites and related rocks» Kornprobst J. (Ed.), Elsevier, 371-382.

HARLEY S.L., HENSEN B.J. and SHERATON J.W. (1990) — *Two-stage decompression in orthopyroxene-sillimanite granulites from Forefinger Point, Enderby Land, Antarctica: implications for the evolution of the Archean Napier Complex*. J. Metamorphic Geol., **8**, 591-613.

IRVING A.J. (1974) — *Geochemical and high pressure experimental studies of garnet pyroxenite and pyroxene granulite xenoliths from the Delegate Basaltic Pipes, Australia*. J. Petrol., **15**, 1-40.

KRETZ R. (1983) — *Symbols for rock-forming minerals*. Am. Mineral., **68**, 277-279.

KROGH E.J. (1988) — *The garnet-clinopyroxene Fe-Mg geothermometer – a reinterpretation of existing experimental data*. Contrib. Mineral. Petrol., **99**, 44-48.

NIMIS P. and ULMER P. (1998) — *Clinopyroxene geobarometry of magmatic rocks. Part 1: An expanded structural geobarometer for anhydrous and hydrous, basic and ultrabasic systems*. Contrib. Mineral. Petrol., **133**, 122-135.

OBATA M. (1994) — *Material transfer and local equilibria in a zoned kelyphite from a garnet pyroxenite, Ronda, Spain*. J. Petrol., **35**, 271-287.

PUNTURO R. and SCRIBANO V. (1997) — *Dati geochimici e petrografici preliminari su xenoliti di clinopirossenite a grana ultragrossa e websteriti nelle vulcanoclastiti mioceniche dell'alta Valle Guffari (Monti Iblei, Sicilia)*. Miner. Petrogr. Acta, **40**, 95-116.

PUNTURO R., KERN H., SCRIBANO V. and ATZORI P. (2000) — *Petrophysical and petrological characteristics of deep-seated xenoliths from the Hyblean Plateau, south-eastern Sicily, Italy: suggestions for a lithospheric model*. Miner. Petr. Acta, **43**, 1-20.

SAPIENZA G. and SCRIBANO V. (2000) — *Distribution and representative whole-rock chemistry of deep-seated xenoliths from the Iblean Plateau, south-eastern Sicily, Italy*. Per. Mineral., **69**, 185-204.

SELVERSTONE J. (1982) — *Fluid inclusions as petrogenetic indicators in granulite xenoliths, Pali-Aike volcanic field, southern Chile*. Contrib. Mineral. Petrol., **79**, 1-9.